[redacted]CLASSIFIED

LARGE-SCALE LOW-SPEED WIND-TUNNEL TESTS OF A DELTA WINGED SUPERSONIC TRANSPORT MODEL TO DETERMINE AERODYNAMIC EFFECTS OF FORWARD OR REVERSE THRUST

By William H. Tolhurst and Kiyoshi Aoyagi

Ames Research Center
Moffett Field, Calif.

NATIONAL AERONAUTICS AND SPACE ADMINISTRATION

[redacted]CONFIDENTIAL

LARGE-SCALE LOW-SPEED WIND-TUNNEL TESTS OF A DELTA WINGED SUPERSONIC TRANSPORT MODEL TO DETERMINE AERODYNAMIC EFFECTS OF FORWARD OR REVERSE THRUST*

By William H. Tolhurst and Kiyoshi Aoyagi

Ames Research Center
Moffett Field, Calif.

SUMMARY

The purpose of the investigation was to determine the aerodynamic effects of the operation of wing-pod-mounted jet engines on the longitudinal characteristics of a supersonic transport model with a delta wing of aspect ratio 2.17.

Data are presented for various configuration combinations which included wing trailing-edge flap deflections from 0° to 30°, horizontal-tail incidence angles from 0° to -15°, and droop angles from 0° to -25°. The airplane angle-of-attack range extended from -4° to $+17^{\circ}$ with a Reynolds number range from 17.2×10^{6} to 32.2×10^{6}. The data include longitudinal force and moment data with the engines in both forward and reverse thrust and the maximum temperature of the surface of the horizontal tail.

The results indicate that with the engines in forward thrust, the aerodynamic effects of engine operation on the lift and pitching-moment characteristics of the airplane were small compared to the direct engine thrust forces. With the engines in reverse thrust the effects on the aerodynamic characteristics were greater than the direct engine thrust forces. Full reverse thrust caused a reduction in longitudinal stability when the wing trailing-edge flaps were undeflected and a loss in stability when the flaps were deflected to 30°.

Under conditions where the horizontal tail would be drooped into the engine exhaust-gas flow field, its skin temperature may increase to approximately 35 percent of the difference between the engine jet-exhaust temperature and free-stream temperature.

INTRODUCTION

Several investigations have been made at the Ames 40- by 80-Foot Wind Tunnel to determine, at large scale, the low-speed aerodynamic characteristics

*Title, Unclassified

of a delta-winged supersonic transport airplane configuration without engines. The results of these tests are reported in references 1, 2, and 3. The horizontal tail considered in reference 3 would be used for longitudinal stability and control during subsonic flight. However, just prior to supersonic flight the tail would be drooped to provide additional directional stability at supersonic speed. It would also provide a means of reducing the effect of the aerodynamic center variation between subsonic and supersonic speeds and give relatively low trim drag throughout the speed range, as reported in reference 4.

The present tests were made to determine the effect of engine operation on the static longitudinal stability of the airplane in configurations representative of take-off and subsonic climb. Tests were also made to determine the effect of full reverse thrust on the static longitudinal characteristics of the airplane in configurations representative of letdown from altitude at subsonic speeds and during the landing approach.

The longitudinal force and moment data of this report show the aerodynamic effects of various values of forward or reverse thrust on the model with several combinations of wing flap deflection and horizontal-tail incidence and droop angles. Also presented is a brief survey of the skin temperatures of the horizontal tail as it was drooped through the exhaust jet.

NOTATION

A_i engine inlet area (total of 4 engines - 5.58 ft^2)

b wing span, ft

c chord length, ft

$\bar{c}$ mean aerodynamic chord, $\frac{2}{S}\int_0^{b/2} c^2\,dy$

C_D drag coefficient, $\frac{\text{drag}}{q_\infty S}$

C_L lift coefficient, $\frac{\text{lift}}{q_\infty S}$

C_m pitching-moment coefficient, $\frac{\text{pitching moment}}{q_\infty S\bar{c}}$

F_g gross thrust of four engines, lb

F_{g_R} gross reverse thrust of four engines, lb

F_n net thrust of four engines, $F_g - \frac{W_e V}{g}$, lb

g gravitational acceleration, 32.2 ft/sec^2

i_t horizontal-tail incidence, positive with trailing edge down, deg

q_∞ tunnel free-stream dynamic pressure, lb/ft^2

S wing area, ft^2

T temperature, ^oR

V tunnel free-stream velocity, ft/sec

W_e engine inlet weight rate of flow, lb/sec

α angle of attack of wing chord plane, deg

Γ_t horizontal-tail dihedral, deg

δ_f wing trailing-edge flap deflection, deg

η wing semispan station, $\frac{\text{spanwise distance}}{b/2}$

Subscripts

E jet engine exhaust tail pipe

t horizontal tail

W wing

∞ tunnel free stream

MODEL

Figure 1 shows the model installed in the wind tunnel and figure 2(a) gives the general arrangement and geometry of the model.

The fuselage was cylindrical with an ogive nose and tail. The diameter of the fuselage where it subtended the wing center line was 4.06 ft. The fineness ratio was 16.6.

Wing

The wing had an aspect ratio of 2.17 with the leading edge swept back 59^o and trailing edge swept forward 10^o. The airfoil section was hexagonal with 3-percent-chord maximum thickness between the 30- and 70-percent-chord points

and a straight line taper from these points to the leading and trailing edges. The leading-edge radius was 0.008 inch and the trailing edge, 0.074 inch.

The trailing-edge flaps were 15-percent chord extending from 13 to 90 percent of the wing semispan. The flaps could be deflected to 30°, except for the sections above the nacelles, which could be deflected to only 5°.

Horizontal Tail

The axis of rotation of the all-movable horizontal tail was the quarter-chord point of the mean aerodynamic chord; the incidence-angle range was 0° to -15°. The tail droop was obtained by rotation about longitudinal axes located in the chord plane of the wing 8.0 inches outboard of the fuselage center line. The tail droop angles ranged from 0° to -25°. Both the horizontal and vertical tails had the same airfoil section as the wing. Thermocouples were imbedded in the upper surface skin close to the leading edge to indicate the temperature rise as the tail was drooped through the exhaust jet of the inboard motors. The thermocouples were located on a constant chord line 0.040 $\bar{c}_t$ back from the leading edge at spanwise stations 0.29, 0.44, 0.60, and 0.76.

Engines and Nacelles

Jet thrust was provided by four YJ-85 GE-5 engines mounted individually in nacelles attached directly to the lower surface of the wing. The inlets were straight ducts of double wall construction, the inside diameter being the same as that of the compressor face. The inlet lip was bevelled and had a leading-edge radius of 0.06 inch.

The thrust reversers were of the cascade type as shown in detail in figure 2(b). Several of the bays were blocked off, both to reduce the open area of the reversers and to direct the hot gas flow away from the engine support structure. The vane angles were fixed at 55° measured from a line normal to the engine thrust axis. For the forward thrust configurations the thrust reversers were removed and the normal tail pipes substituted.

TESTS AND PROCEDURE

Force and moment data were obtained through an angle-of-attack range from -4° to $+18^{\circ}$. The test Reynolds number ranged from 17.2×10^6 to 32.2×10^6 which corresponded to wind-tunnel free-stream dynamic pressures from 25 to 100 pounds per square foot. The total gross thrust from all four engines was varied from 6,230 pounds in forward thrust to 1,770 pounds in reverse thrust. The reverse thrust efficiency varied between 42 and 52 percent of the forward gross thrust.

The forward thrust of each engine was calibrated statically against the intake weight rate of flow to obtain net thrust with forward velocity. The drag due to the reverse thrust of each engine was calibrated against inlet weight rate of flow with the wind-tunnel free-stream dynamic pressure at 10 pounds per square foot. These data were then corrected for airplane drag and ram drag to obtain reverse gross thrust.

The airplane aerodynamic data were obtained at various angles of attack but with constant engine inlet weight rate of flow and wind-tunnel dynamic pressure. The data for no thrust were obtained with the engine inlets plugged.

CORRECTIONS

The following wind-tunnel wall corrections were applied to the force and moment data:

$$\Delta\alpha = 0.994\ C_L$$

$$\Delta C_D = 0.01735\ C_L^2$$

$$\Delta C_m = -0.00939\ C_L$$

The intake weight rate of flow and engine thrust were corrected to standard atmospheric conditions. The force data are referred to the wind axes system with moments taken about the quarter-chord point of the mean aerodynamic chord.

RESULTS

Table I is an index of the configurations tested during this investigation and the figure numbers to which they apply.

The data are presented at constant values of the ratio $F_g/q_\infty S$, as presented in reference 5, and in forward thrust also in terms of the parameter $F_n/q_\infty A_i$ which is discussed later.

Figure 3 shows the effect of tail droop, without engine operation, on the longitudinal characteristics of the model.

Figure 4 presents the effect of engine operation, at several values of thrust, on the longitudinal characteristics of the basic model where $\Gamma_t = 0^\circ$ and $i_t = -5^\circ$.

Figure 5 presents the effect of engine thrust with the horizontal tail at several angles of droop. Figure 6 shows the effect of increased free-stream dynamic pressure with engine thrust increased to obtain values of

$F_n/q_\infty A_i$ similar to those in figure 5(b) with the same model configuration. Figure 7 shows the longitudinal characteristics of the model at nearly the same values of $F_n/q_\infty A_i$ for the same model configuration as that of figure 5(b) except with the horizontal tail at 0° incidence angle.

The longitudinal characteristics of the model with the wing trailing-edge flaps deflected to 10°, 20°, and 30° are presented in figures 8(a), (b), and (c), respectively.

Figure 9 presents the variation in temperature ratio of the maximum recorded horizontal-tail skin temperature to jet engine exhaust tail-pipe temperature with change in the thrust parameter $F_n/q_\infty A_i$ for the tail droop angles tested.

Figures 10 through 13 show the effect of reverse thrust on the longitudinal characteristics of the model. Figures 10 and 11 present data with the horizontal tail undrooped at a free-stream dynamic pressure of 50 and 25 pounds per square foot, respectively. Figure 12 presents data with the tail drooped -15°. Figure 13 shows results obtained with the wing flaps deflected 30° and the tail undrooped at two tail incidences.

Figure 14 shows the variation of pitching moment with change in $F_n/q_\infty A_i$ at several values of q_∞ and Γ_t. Figure 15 shows the variation of pitching-moment increment at $\alpha = 0^\circ$ due to change in $F_n/q_\infty A_i$ along with calculated engine thrust contribution to the pitching-moment increment at several flap deflection angles.

Figure 16 shows the pitching-moment increment due to variation of reverse thrust $F_g/q_\infty S$ for flaps undeflected and deflected 30°. Calculated pitching-moment increments due to reverse thrust are also presented in the figure.

DISCUSSION

Correlation Parameter $F_n/q_\infty A_i$

The parameter $F_g/q_\infty S$ was introduced in reference 5 to enable correlation of the effects of engine thrust reversal on the aerodynamic characteristics of an airplane over a range of thrust and velocity. In order to correlate the effects of forward thrust on the airplane characteristics in the present investigation the parameter $F_n/q_\infty A_i$ is used which is the ratio of the change of the momentum of the net forward thrust to the momentum of the free-stream air flow into the engines.

In figure 14 the results from figures 4, 5, and 6 are compared in terms of the variation of pitching moment with momentum ratio $F_n/q_\infty A_i$; reasonable correlation exists over the range of thrust and dynamic pressures investigated. It therefore appears that the parameter should be usable in determining the effects of thrust on the characteristics of a full-scale airplane from

those of a large-scale model presented herein by relating the results with this correlation factor as follows,

$$\left(\frac{F_n}{q_\infty A_i}\right)_{Model} = \left(\frac{F_n}{q_\infty A_i}\right)_{Airplane}$$

Forward Thrust

In general, figures 4 through 8 show little aerodynamic effect on the longitudinal characteristics of the model other than that produced by the direct thrust forces of the engines. However, with the flaps deflected 10° (fig. 15), the calculated pitching-moment increment, ΔC_m, due to direct thrust was greater than the total measured ΔC_m, indicating that the flow field induced by the engine exhaust increased the pitch-down moment due to flap deflection. This was true also for $\delta_f = 20°$ and 30° at low values of $F_n/q_\infty A_i$, but at the higher values, the induced flow field changed so that the measured ΔC_m is greater than the calculated direct thrust contribution.

With the horizontal tail drooped 0°, -15°, or -25°, the jet exhaust had essentially no effect on the static longitudinal stability throughout the angle-of-attack range investigated (fig. 5).

Horizontal-Tail Skin Temperatures

Figure 9 shows the variation of the maximum horizontal-tail skin temperature with change in values of $F_n/q_\infty A_i$ for tail droop angles of 0°, -15°, and -25°. The tail temperatures are represented by the ratio $T_t - T_\infty / T_E - T_\infty$. Undrooped, the horizontal tail was above the exhaust jet and the skin temperature was only slightly higher than free-stream temperature even at $F_n/q_\infty A_i = 14$, the approximate value for take-off at 160 knots. Drooped -15°, the tail was close to the center of the exhaust jet, and at $F_n/q_\infty A_i = 14$ the tail temperature increase was approximately 60 percent of the increment of temperature between the tunnel free stream and the exhaust jet.

At high subsonic Mach number where the horizontal tail would be drooped through the exhaust prior to supersonic flight, the value of $F_n/q_\infty A_i$ would be approximately 2.0 at a Mach number of 0.9 at 40,000 feet. To the extent that $F_n/q_\infty A_i$ can be considered a correlating parameter for temperature when based on the data of figure 9, the resulting temperature rise would be about 35 percent of the difference between free-stream and jet-exhaust temperatures. With the horizontal tail drooped to -25°, the temperature rise was considerably less than at -15° droop since the tail was again outside of the jet-exhaust stream.

Reverse Thrust

The entire reverse-thrust portion of the investigation was conducted with the engines operating at full reverse thrust. The resulting aerodynamic effects on the pitching moment were large.

The data presented in figures 10 and 11 indicate that with the wing trailing-edge flaps undeflected there was a C_m shift in the negative direction which was opposite to and of much greater magnitude than the shift caused by forward thrust at comparable values of $F_g/q_\infty S$. In addition to the shift in C_m, there was also a reduction in the stability above $C_L = 0.3$ which was probably due to either a reduction in dynamic pressure or a change in downwash angle at the tail as a result of thrust reversal. Figure 12 shows essentially the same results with the tail drooped to -15°. Figure 13 shows that with the flaps deflected 30°, the reduction in static longitudinal stability was considerably greater than with flaps at 0°.

Figure 15 indicates that at 0° angle of attack the ΔC_m that occurs with the engine operating in forward thrust is due largely to the direct thrust forces and is not greatly affected by flap deflection. In contrast, figure 16 shows that with thrust reversal, the ΔC_m due to engine operation is greater and of opposite direction to that of the forward thrust. The aerodynamic effects are much greater than the effects of the direct reverse thrust forces. Deflecting the flaps to 30° produced only a small change in the pitching moment relative to the values obtained with 0° flap deflection with thrust reversal.

The model as tested was capable of only full forward or full reverse thrust, the thrust being controlled by the engine speed. Therefore, it was not determined whether modulated thrust reversal, as studied in reference 6, would prevent the large changes in longitudinal stability caused by full reverse thrust.

Ames Research Center
National Aeronautics and Space Administration
Moffett Field, Calif., July 7, 1964

REFERENCES

1. Brady, James A., Page, V. Robert, and Koenig, David G.: Large-Scale Low-Speed Wind-Tunnel Tests of a Delta Winged Supersonic Transport Model With a Delta Canard Control Surface. NASA TM X-643, 1962.

2. Koenig, David G., Brady, James A., and Page, V. Robert: Large-Scale Wind-Tunnel Tests at Low Speed of a Delta Winged Supersonic Transport Model in the Presence of the Ground. NASA TM X-644, 1962.

3. Koenig, David G., and Corsiglia, Victor R.: Large-Scale Low-Speed Wind-Tunnel Tests of a Delta Winged Supersonic Transport Model With Various Canard, Horizontal Tail, and Wing Modifications. NASA TM X-857, 1964.

4. Fletcher, LeRoy S.: Static Stability Characteristics of a Delta-Winged Airplane Configuration With Nacelles, a Trapezoidal Canard and a Drooped Tail at Mach Numbers From 0.70 to 3.52. NASA TM X-780, 1963.

5. Tolhurst, William H., Jr., Kelly, Mark W., and Greif, Richard K.: Full-Scale Wind-Tunnel Investigation of the Effects of a Target-Type Thrust Reverser on the Low-Speed Aerodynamic Characteristics of a Single Engine Jet Airplane. NASA TN D-72, 1959.

6. Hickey, David H., Tolhurst, William H., Jr., and Aoyagi, Kiyoshi: Investigation of the Longitudinal Characteristics of a Large-Scale Jet Transport Model Equipped With Controllable Thrust Reversers. NASA TN D-786, 1961.

TABLE I.- MODEL CONFIGURATIONS FOR WHICH THREE-COMPONENT FORCE DATA ARE PRESENTED

Figure	δ_f, deg	Γ_t, deg	i_t, deg	Nominal q_∞, psf	Engine thrust
3	0	0, -15, -25	-5	25	None
4		0			None
					Forward
5(a)		0			None
				50	Forward
5(b)		-15		25	None
				50	Forward
5(c)		-25		25	None
				50	Forward
6		-15		25	None
				100	Forward
7		-15	0	25	None
				50	Forward
8(a)	10	0	-5	25	None
					Forward
8(b)	20				None
					Forward
8(c)	30				None
					Forward
10	0				None
				50	Reverse
11				25	None
					Reverse
12		-15		25	None
				50	Reverse
13(a)	30	0		25	None
					Reverse
13(b)			-15		None
					Reverse

A-30963

Figure 1.- Photograph of the model mounted in the Ames 40- by 80-Foot Wind Tunnel.

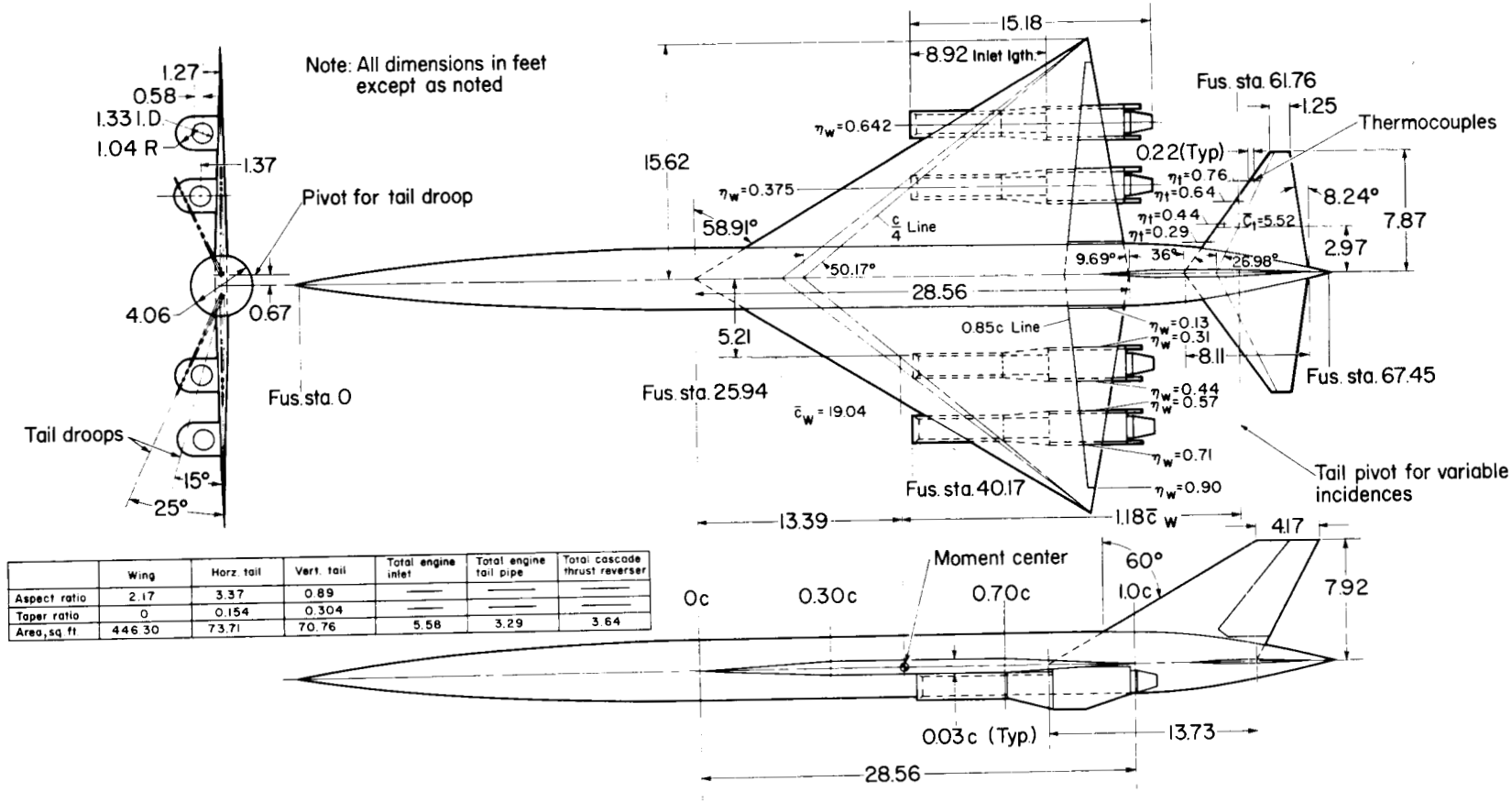

	Wing	Horz. tail	Vert. tail	Total engine inlet	Total engine tail pipe	Total cascade thrust reverser
Aspect ratio	2.17	3.37	0.89	—	—	—
Taper ratio	0	0.154	0.304	—	—	—
Area, sq ft	446.30	73.71	70.76	5.58	3.29	3.64

(a) Geometric details of the model.

Figure 2.- Details of the model.

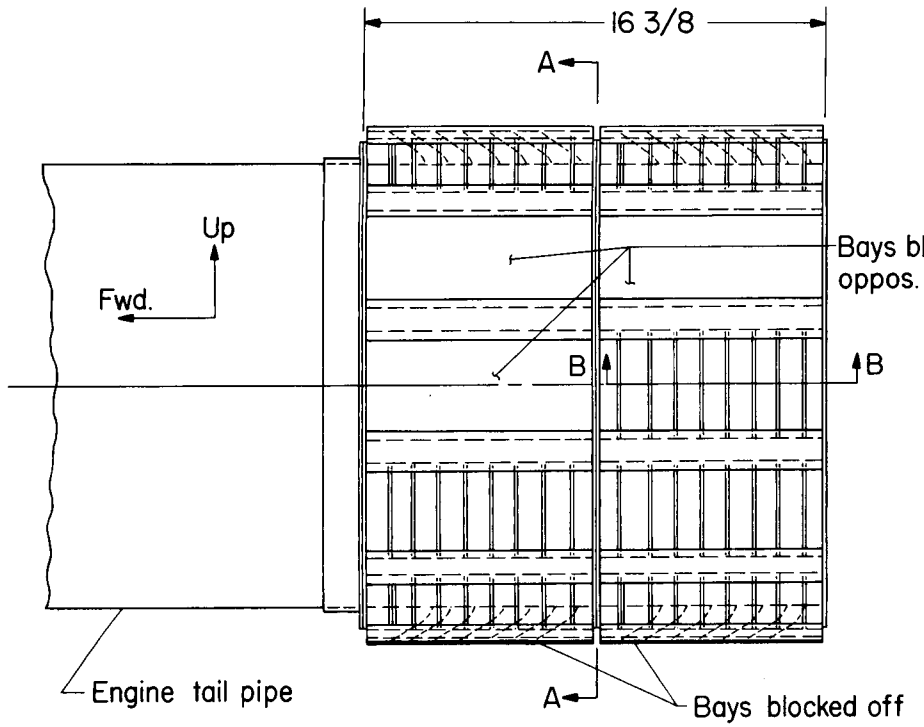

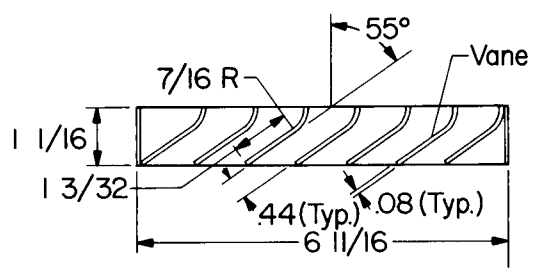

Section B-B

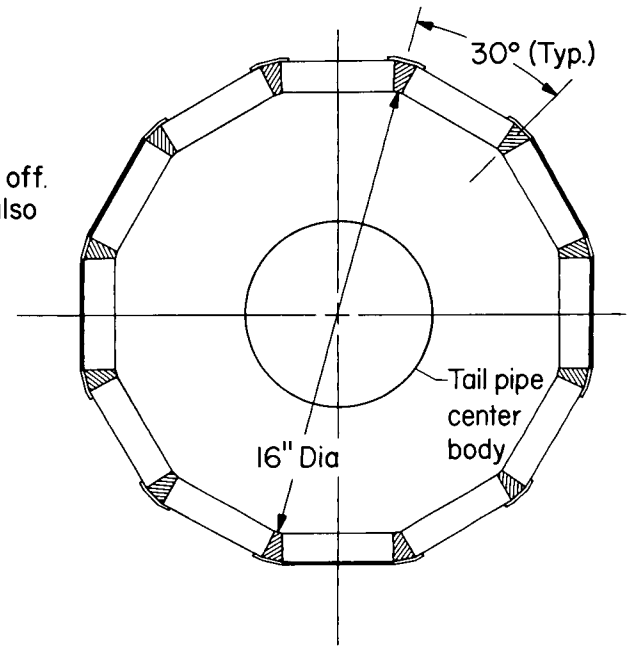

Section A-A

Note: All dimensions in inches
except as noted

(b) Details of the cascade thrust reverser.

Figure 2.- Concluded.

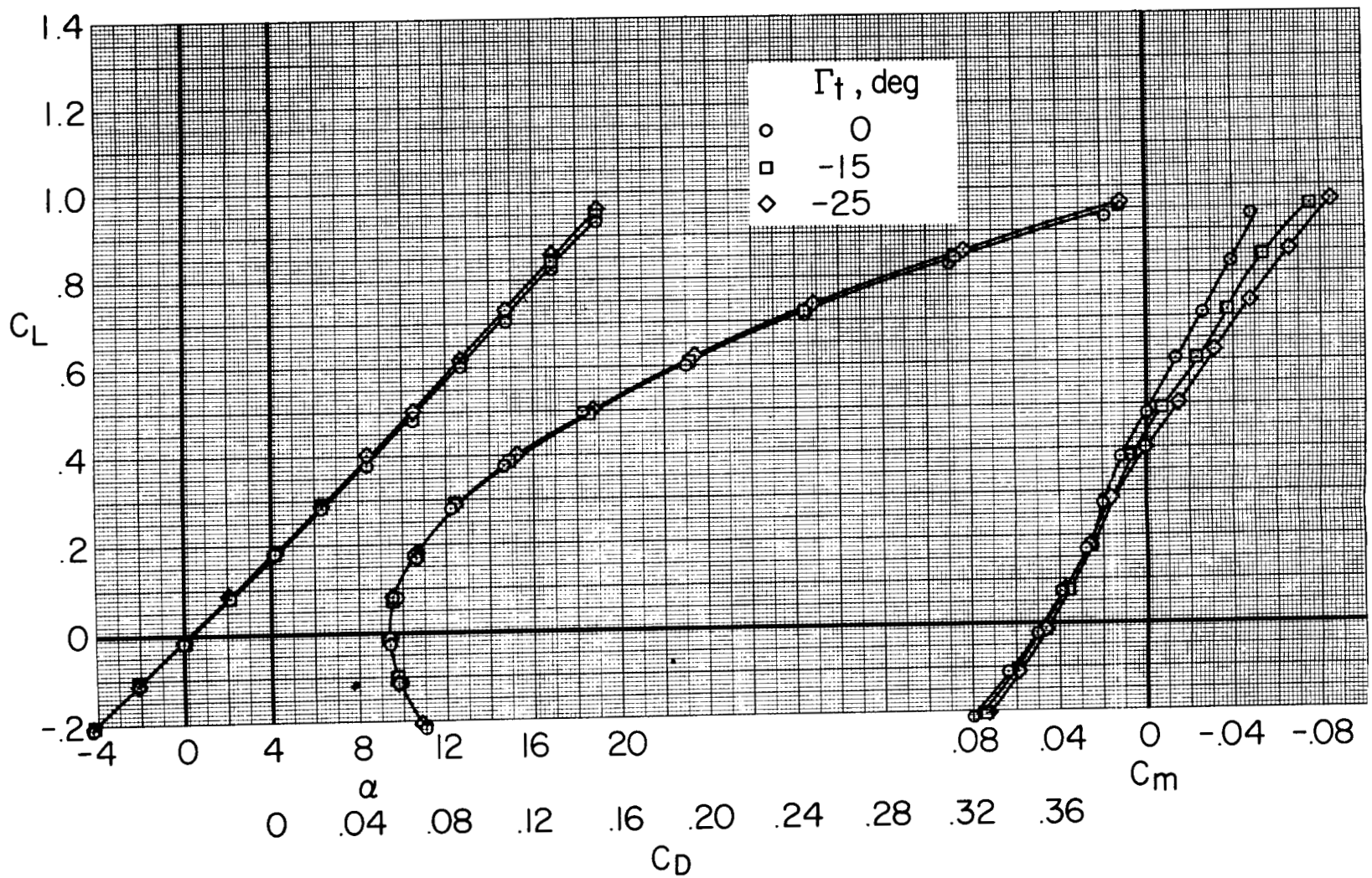

Figure 3.- The effect of tail droop on the longitudinal characteristics of the model with no engine thrust; $\delta_f = 0^\circ$, $q_\infty = 25$ psf, $i_t = -5^\circ$.

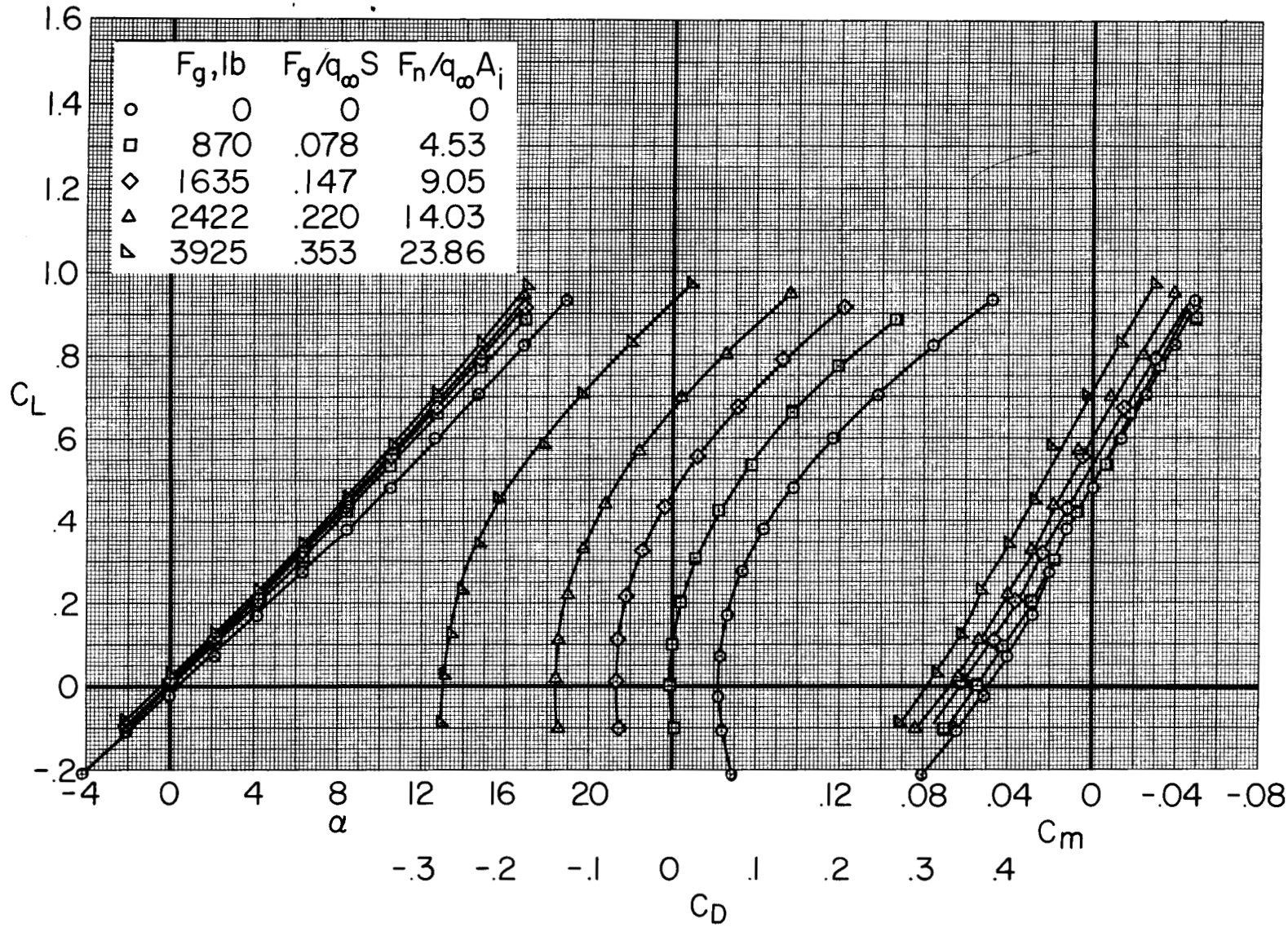

Figure 4.- The effect of engine thrust on the longitudinal characteristics of the model; $\delta_f = 0^o$, $q_\infty = 25$ psf, $\Gamma_t = 0^o$, $i_t = -5^o$.

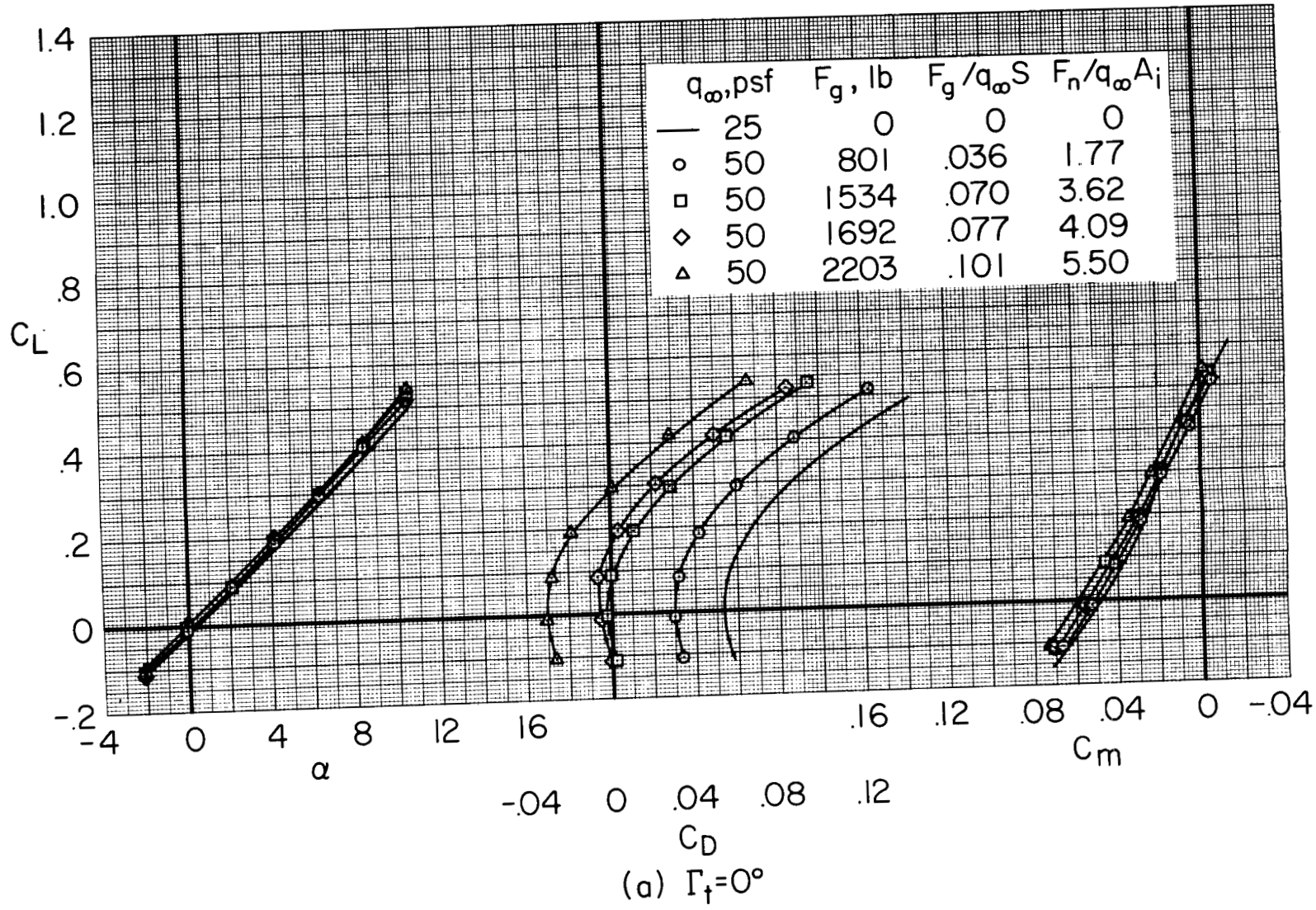

Figure 5.- The effect of engine thrust on the longitudinal characteristics of the model with the horizontal tail at several angles of droop; $\delta_f = 0^\circ$, $i_t = -5^\circ$.

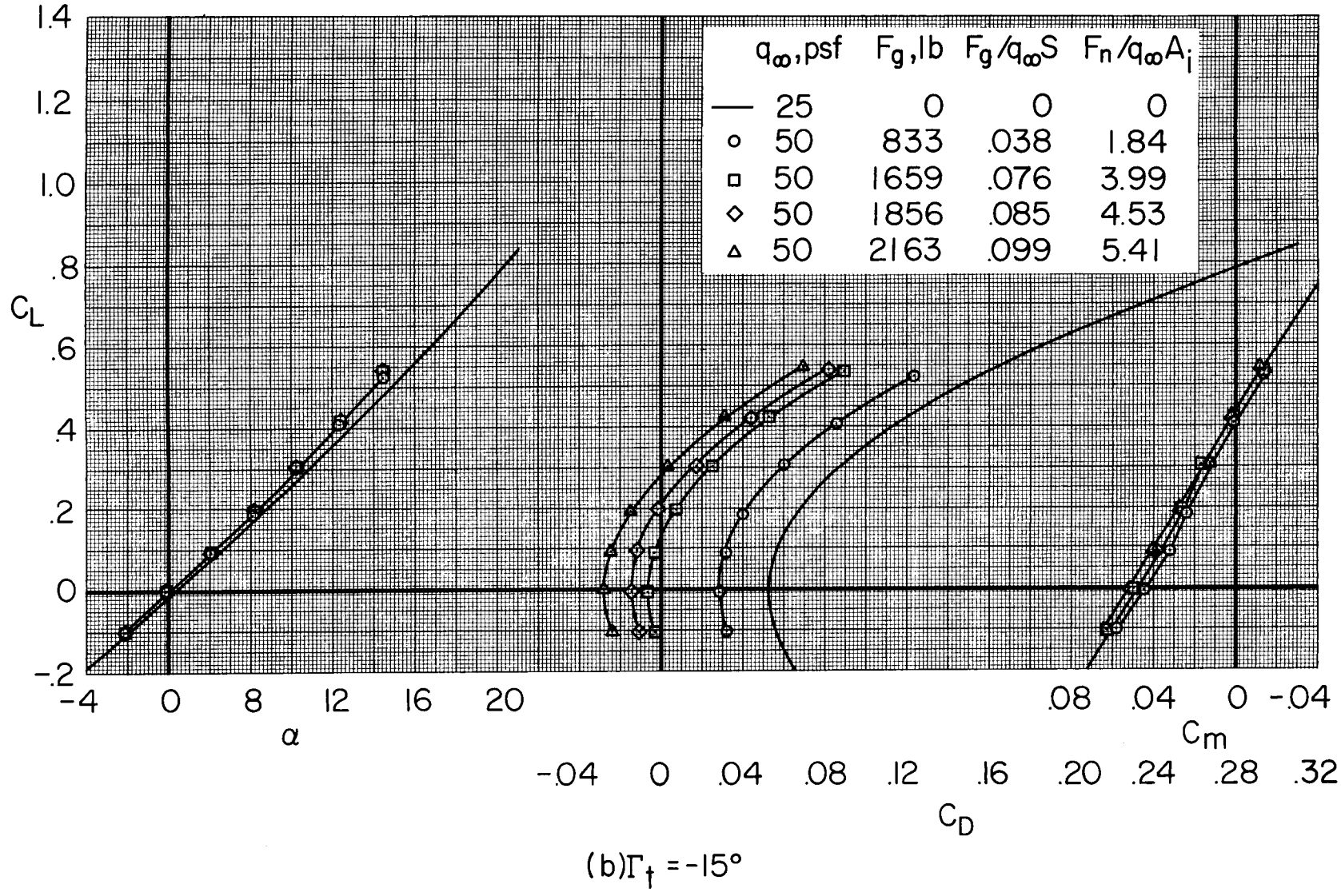

(b) $\Gamma_t = -15°$

Figure 5.- Continued.

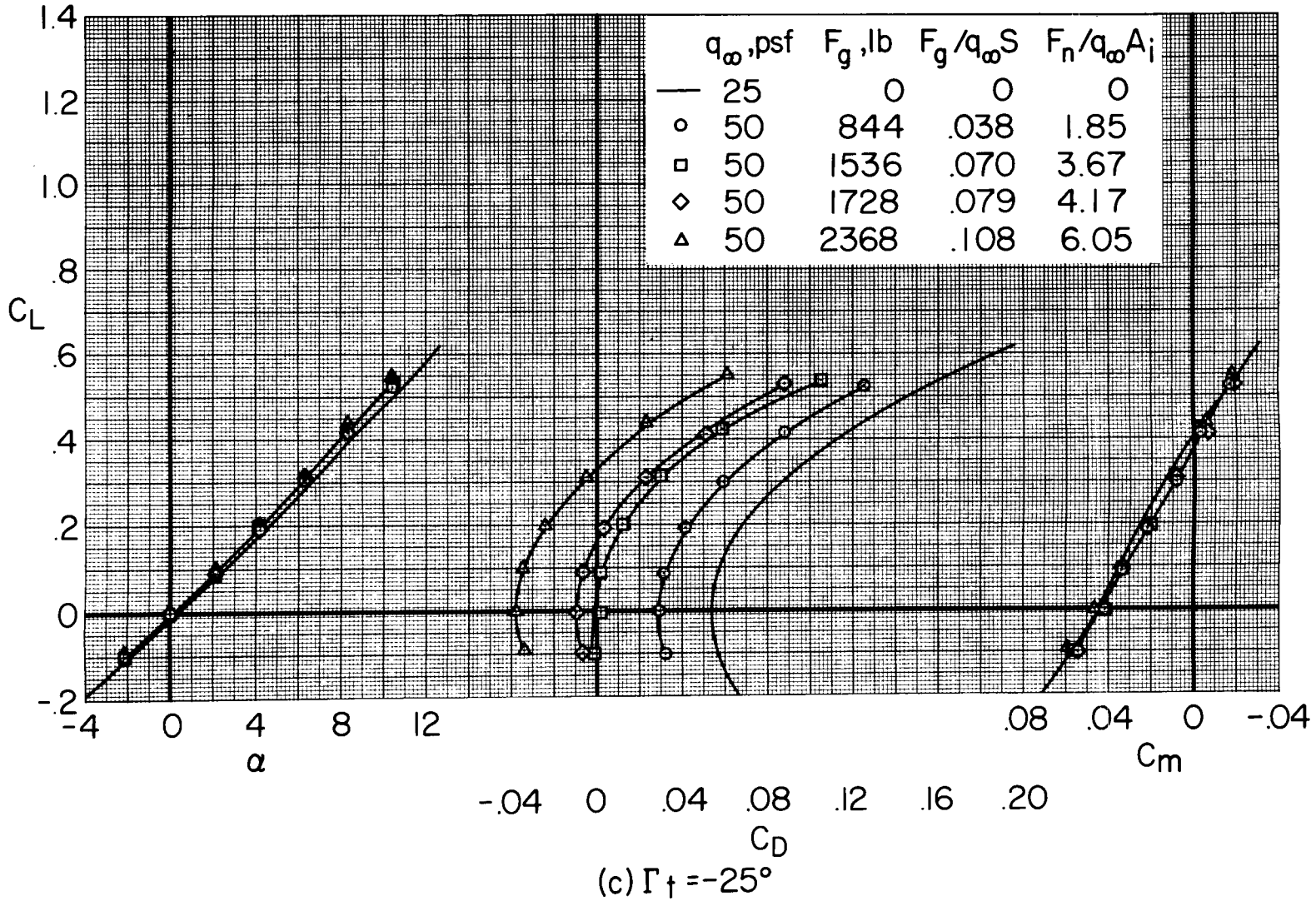

(c) $\Gamma_t = -25°$

Figure 5.- Concluded.

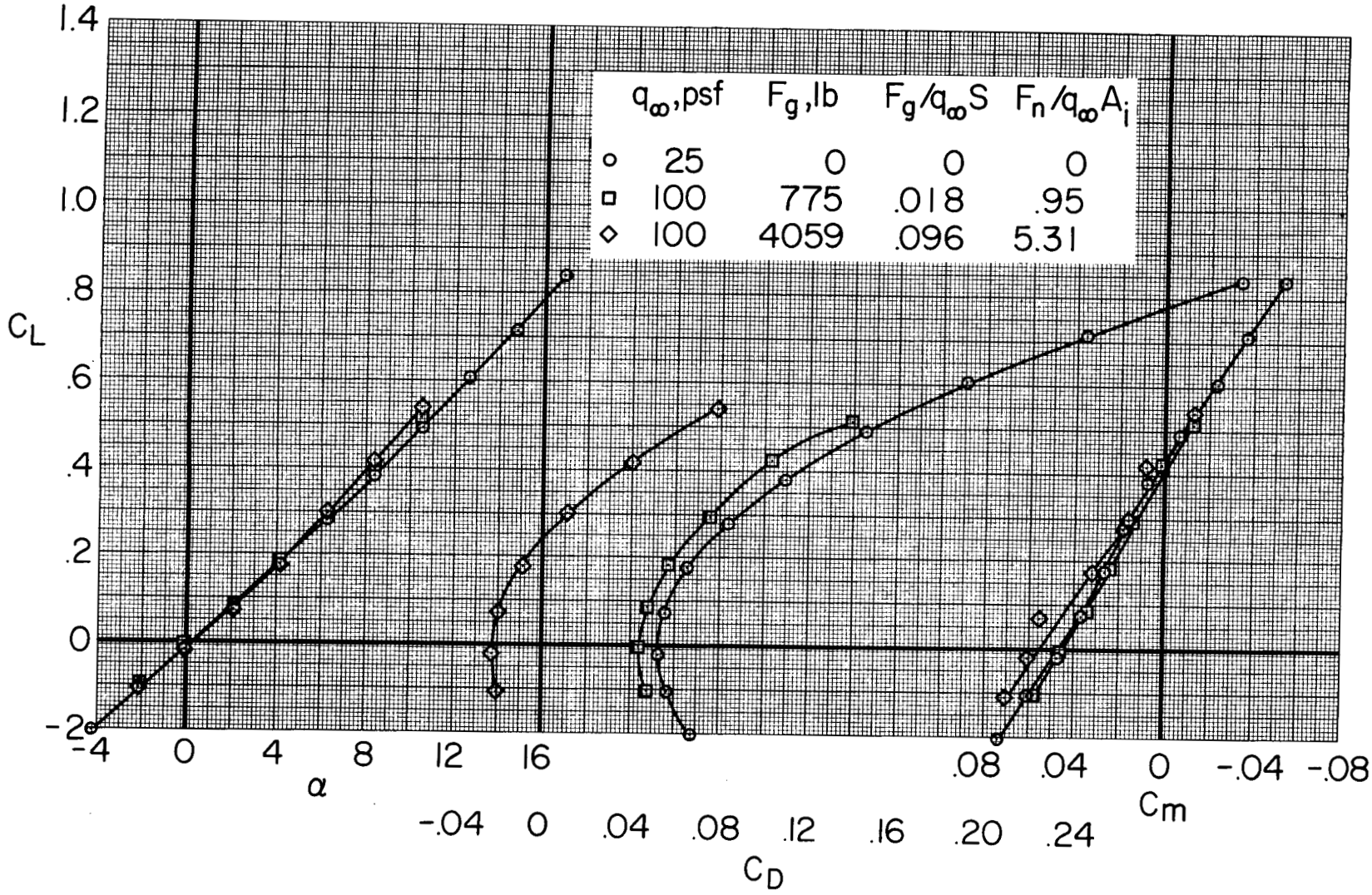

Figure 6.- The effect of engine thrust on the longitudinal characteristics of the model at a nominal free-stream dynamic pressure of 100 psf; $\delta_f = 0^\circ$, $\Gamma_t = -15^\circ$, $i_t = -5^\circ$.

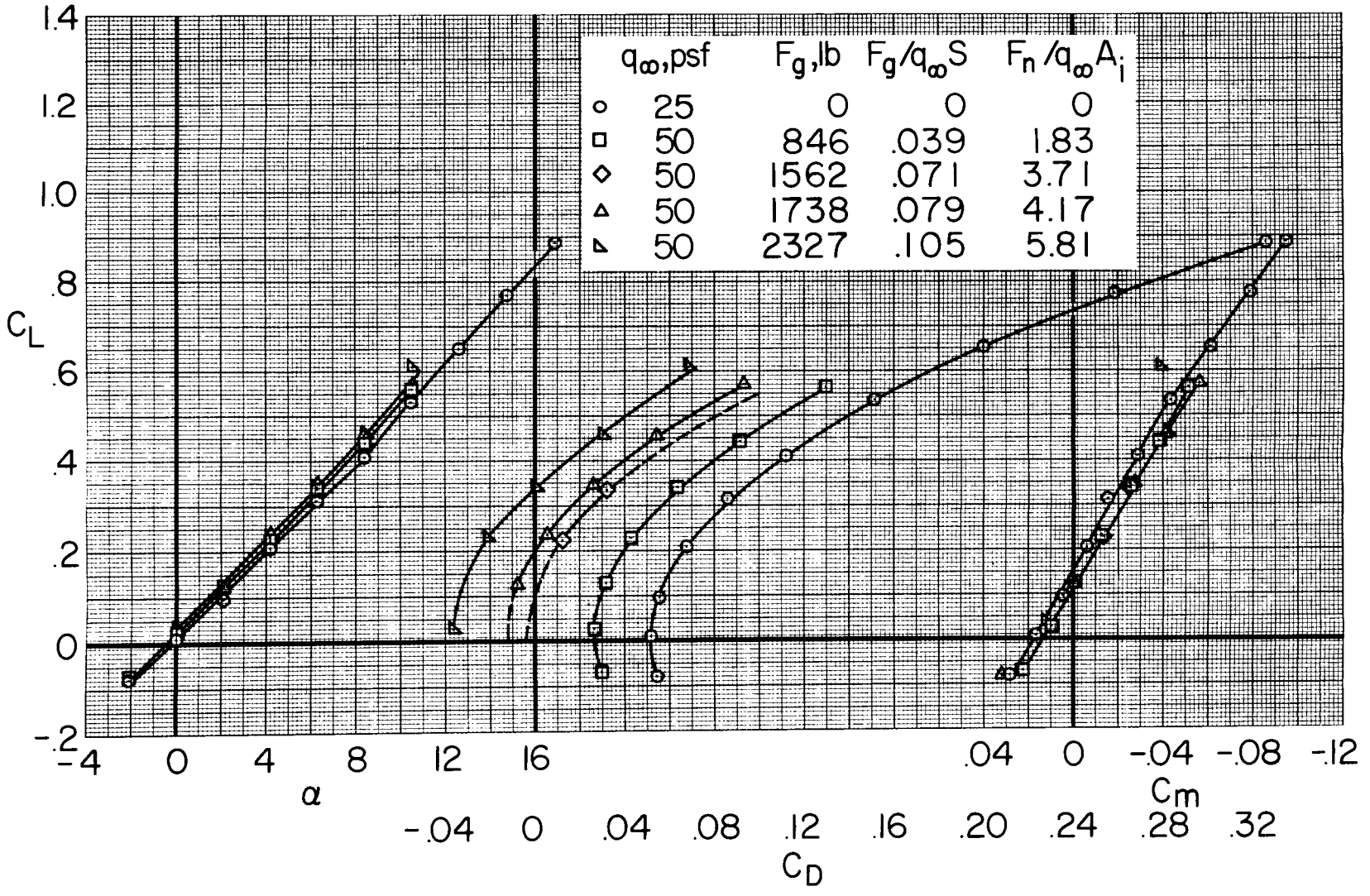

Figure 7.- The effect of engine thrust on the longitudinal characteristics with the horizontal tail at 0° incidence; $\delta_f = 0^\circ$, $\Gamma_t = -15^\circ$.

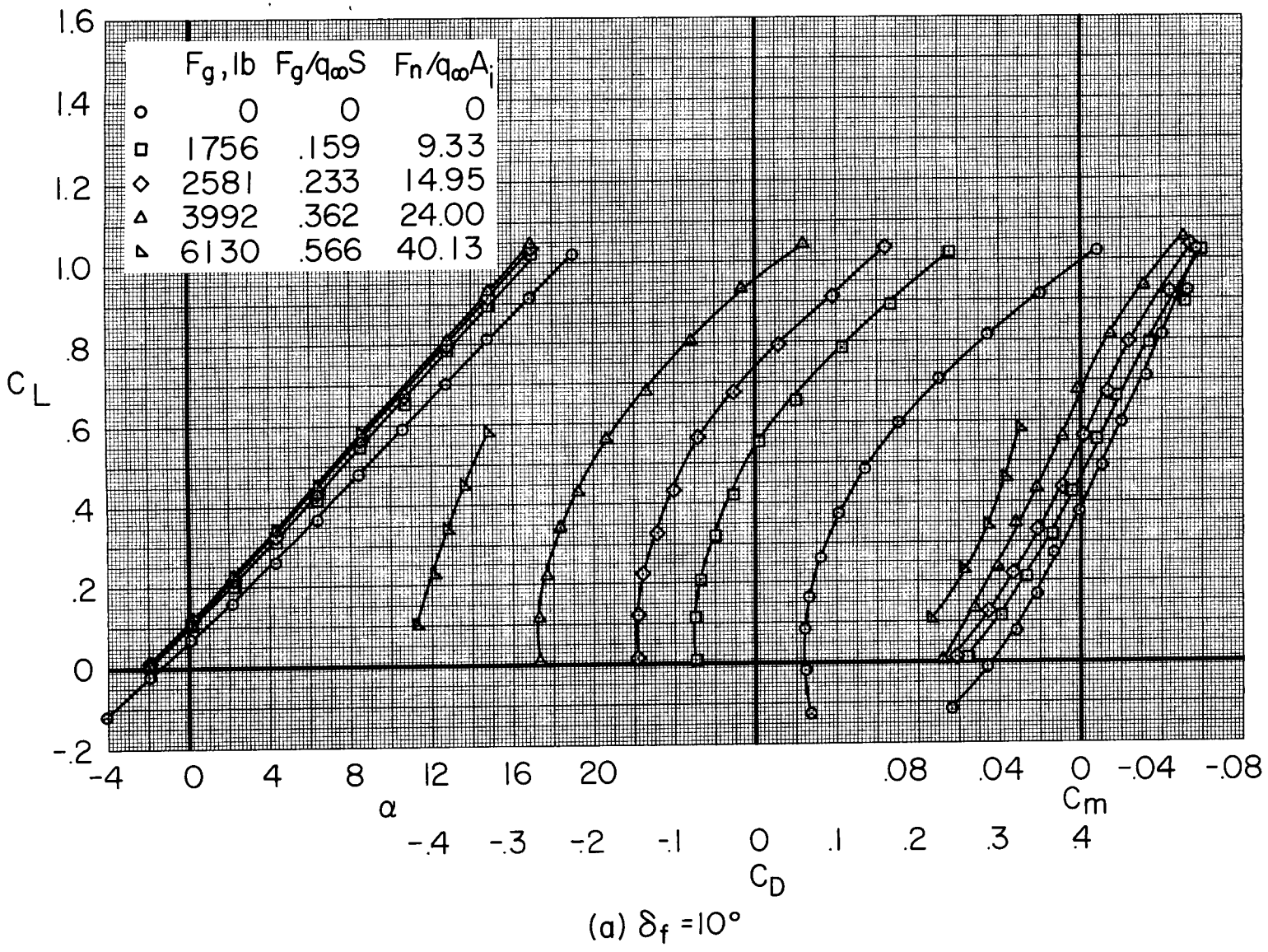

Figure 8.- The effect of engine thrust on the longitudinal characteristics of the model with wing trailing-edge flaps at several deflections; q_∞ = 25 psf, $\Gamma_t = 0°$, $i_t = -5°$.

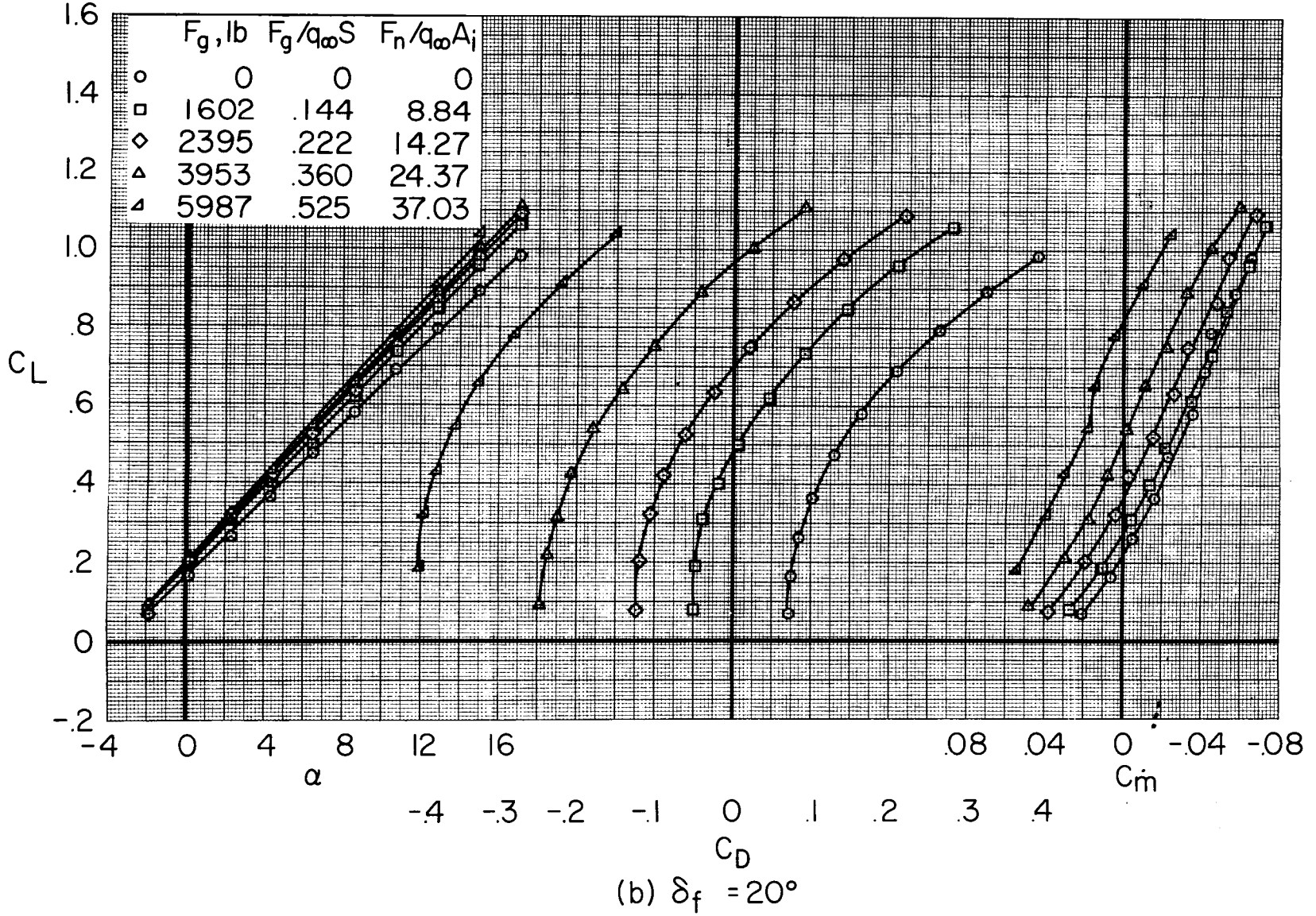

(b) $\delta_f = 20°$

Figure 8.- Continued.

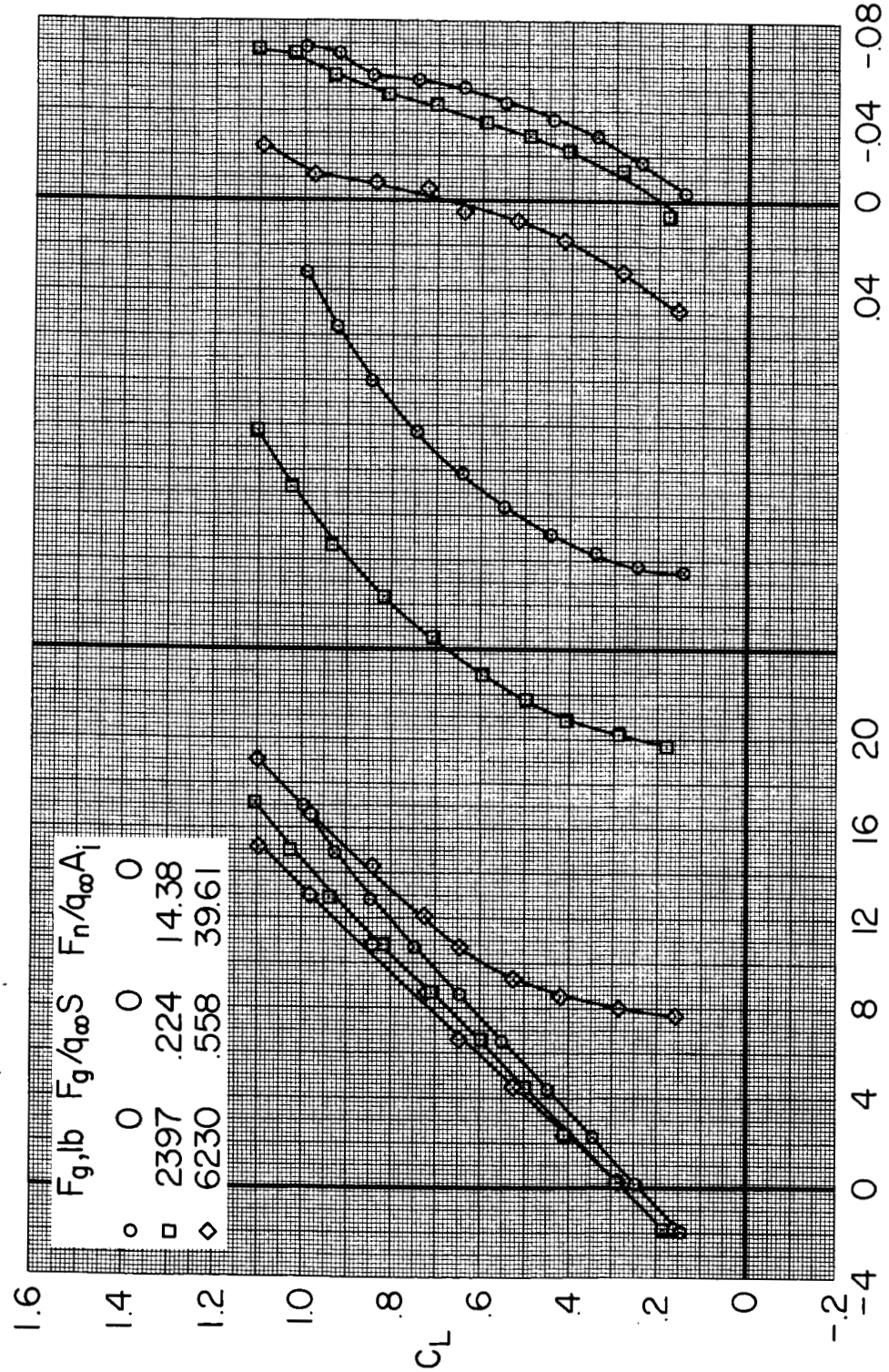

(c) $\delta_f = 30°$

Figure 8.- Concluded.

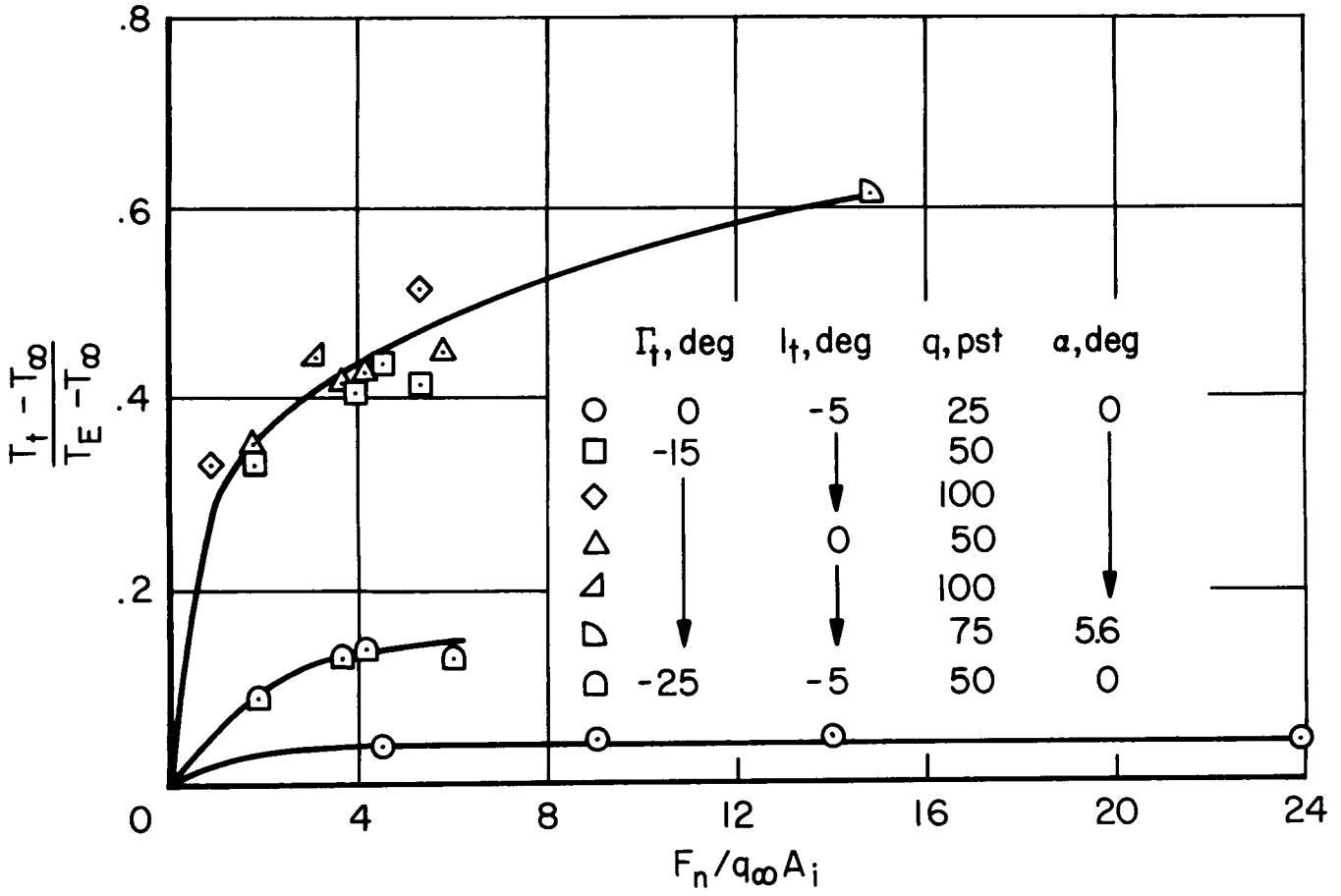

Figure 9.- The variation of the ratio of maximum recorded surface temperature of the horizontal tail to jet engine exhaust temperature with engine thrust at several angles of tail droop; $\delta_f = 0^\circ$.

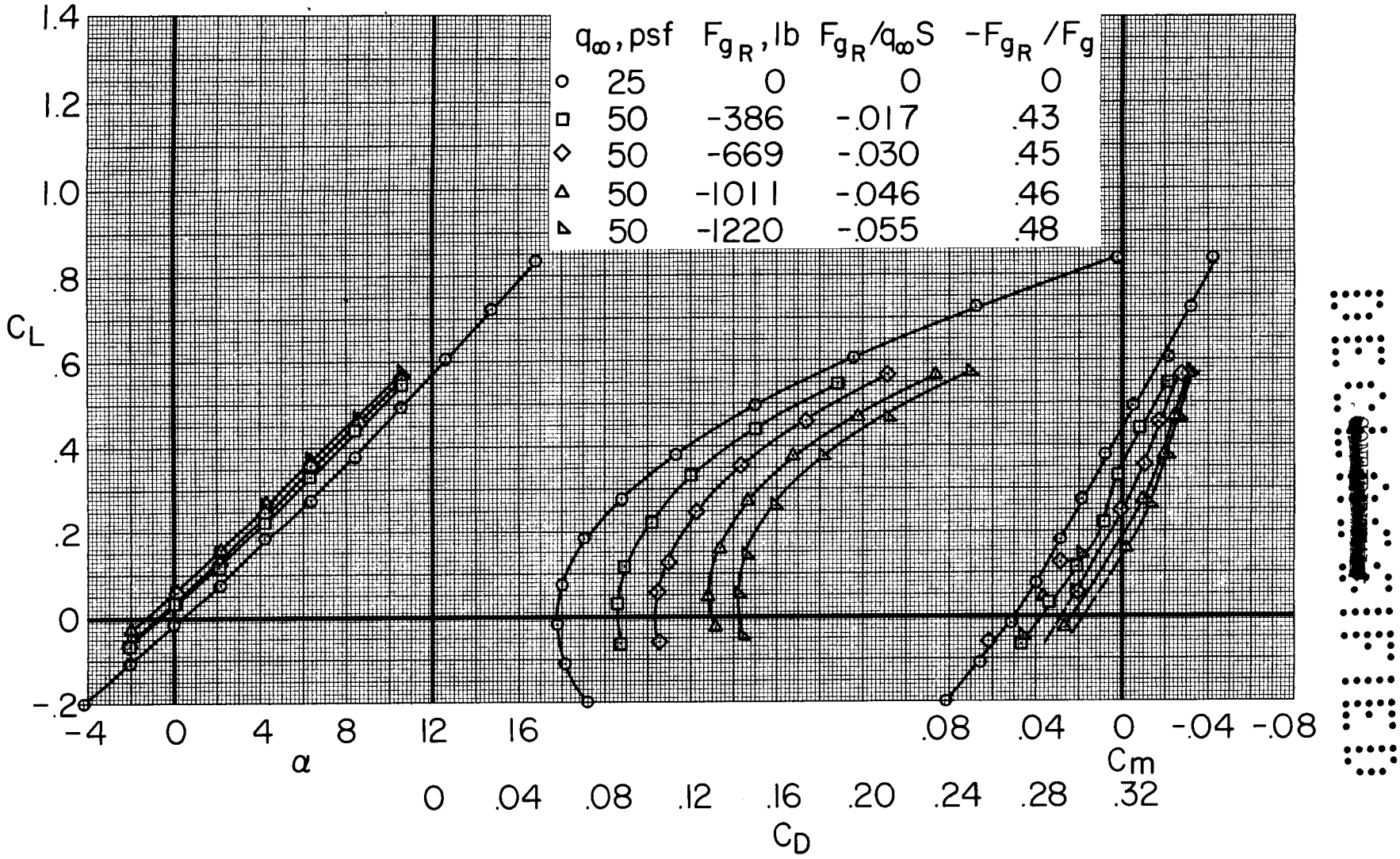

Figure 10.- The effect of reverse thrust on the longitudinal characteristics of the model; $\delta_f = 0^\circ$, $\Gamma_t = 0^\circ$, $i_t = -5^\circ$.

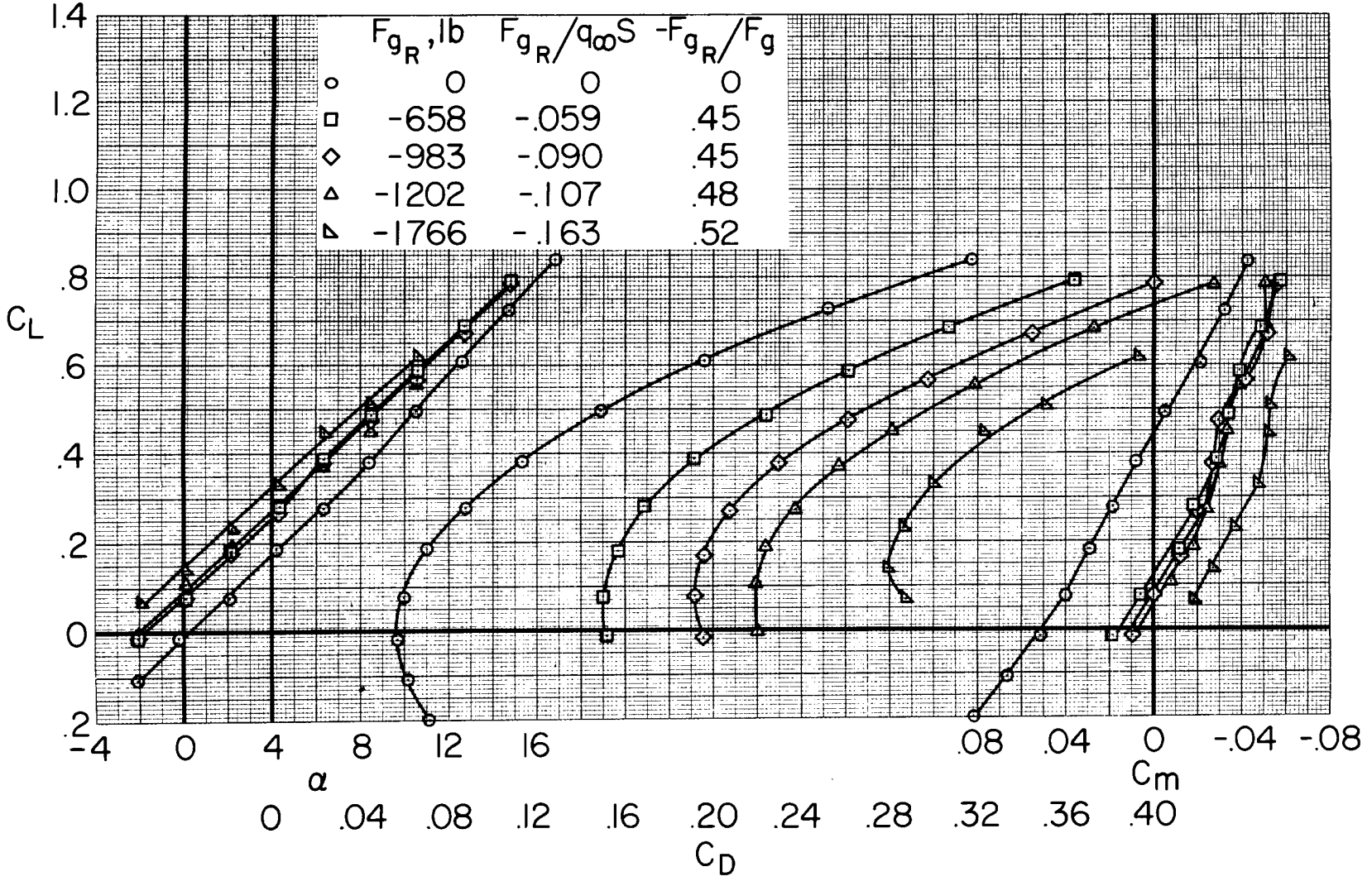

Figure 11.- The effect of reverse thrust on the longitudinal characteristics of the model at a nominal free-stream dynamic pressure of 25 psf; $\delta_f = 0^\circ$, $\Gamma_t = 0^\circ$, $i_t = -5^\circ$.

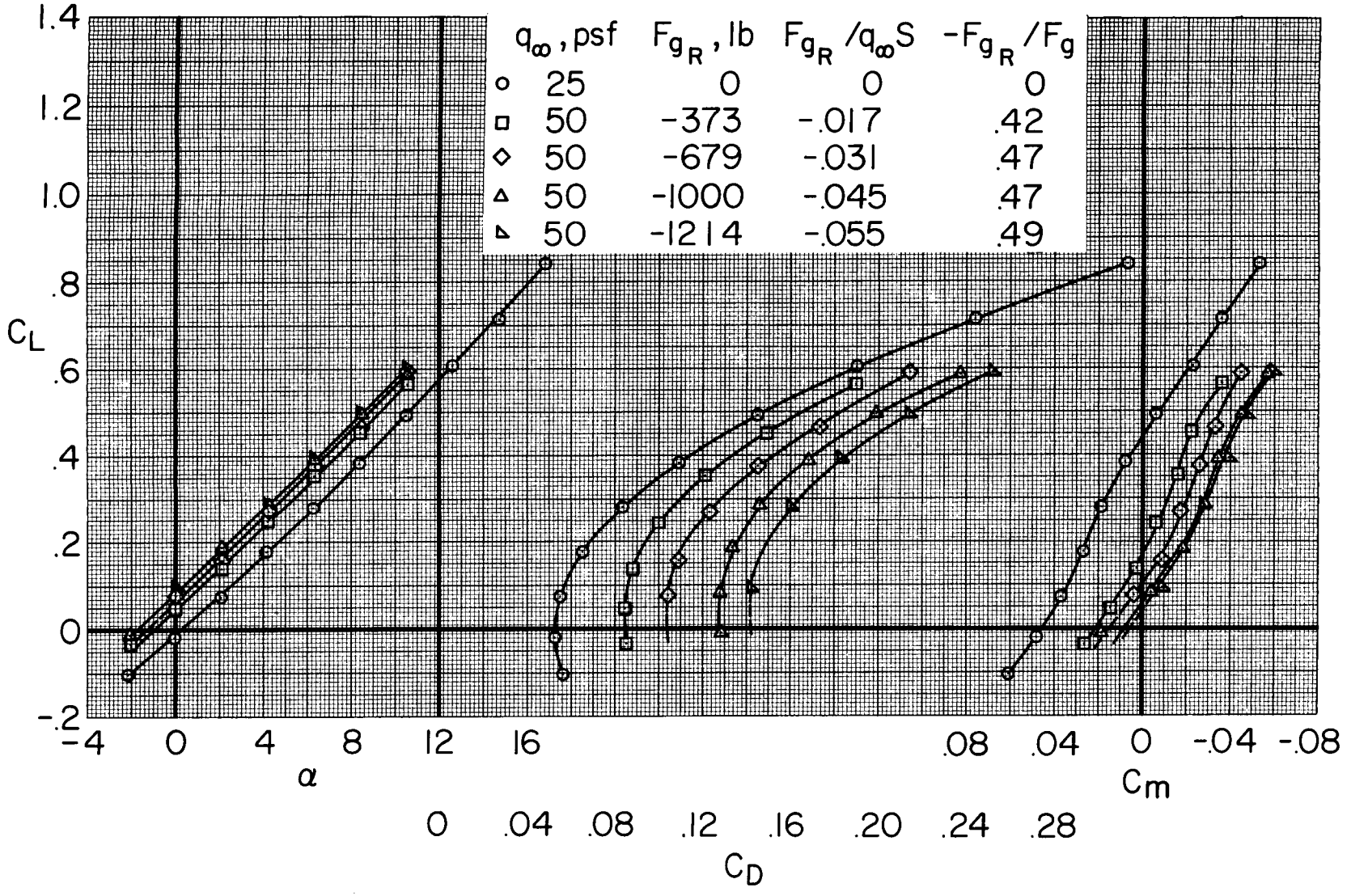

Figure 12.- The effect of reverse thrust on the longitudinal characteristics of the model with the horizontal tail drooped to -15°; $\delta_f = 0°$, $i_t = -5°$.

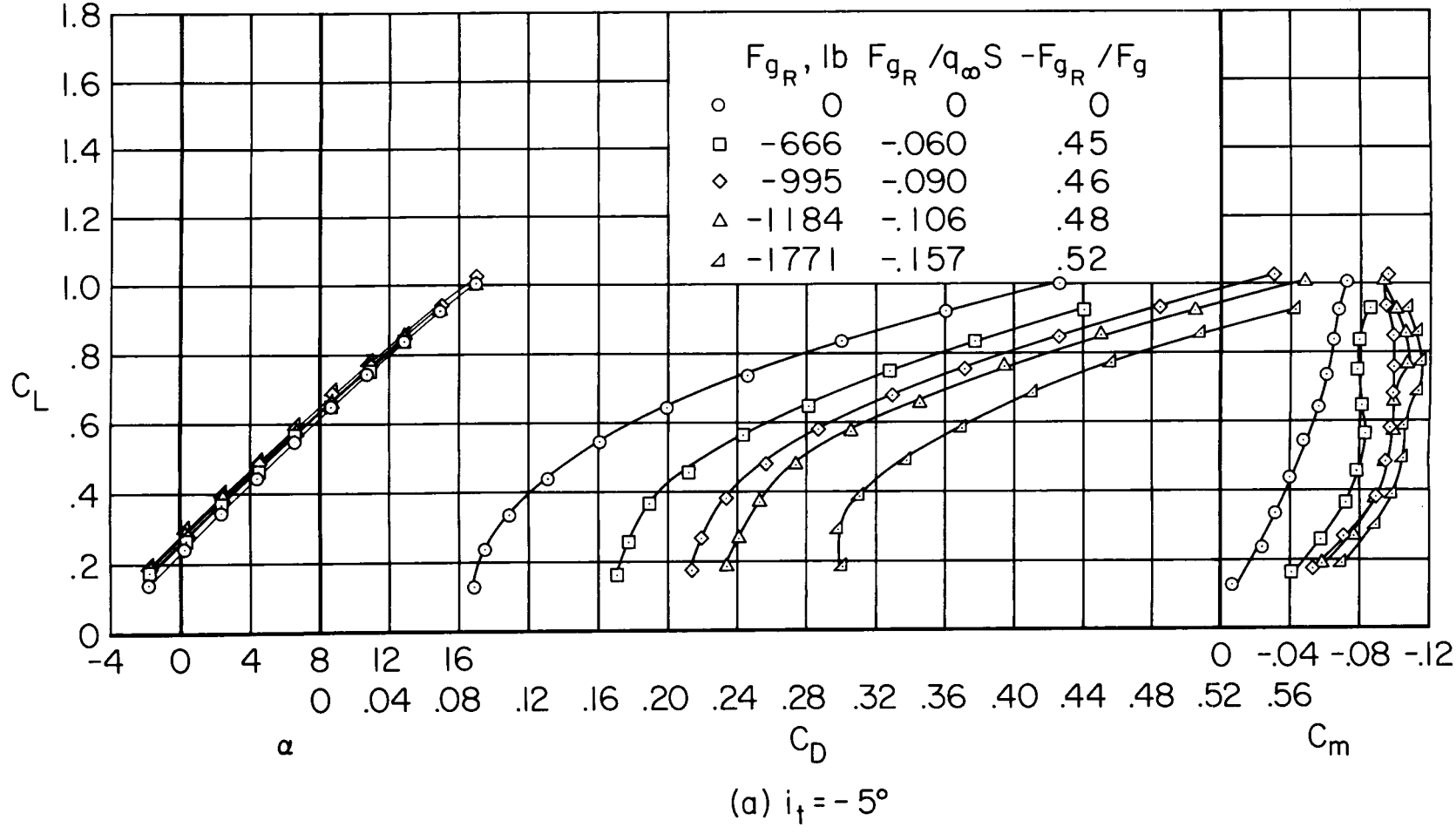

Figure 13.- The effect of reverse thrust on the longitudinal characteristics of the model with wing trailing-edge flaps deflected 30°; q_∞ = 25 psf, Γ_t = 0°.

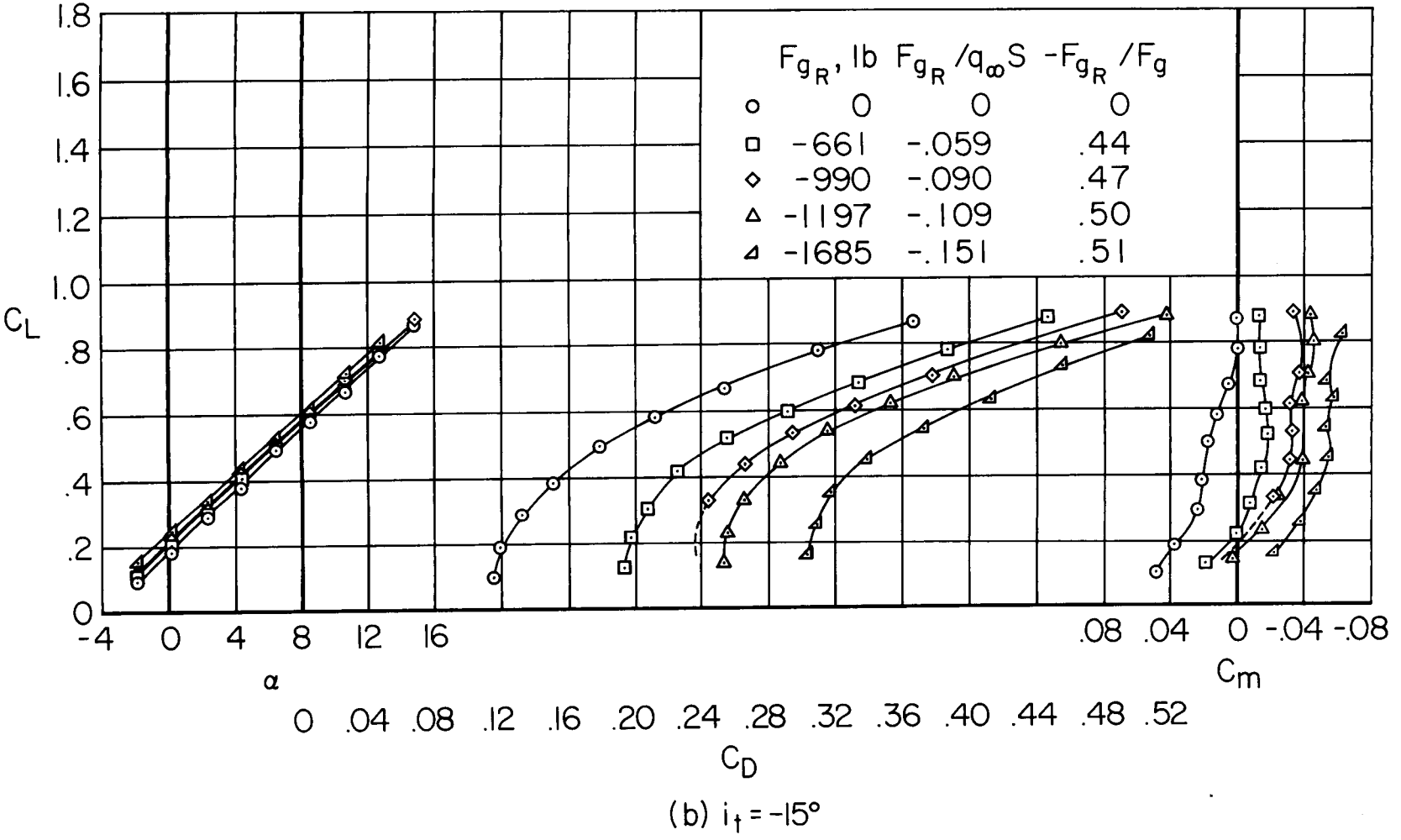

(b) $i_t = -15°$

Figure 13.- Concluded.

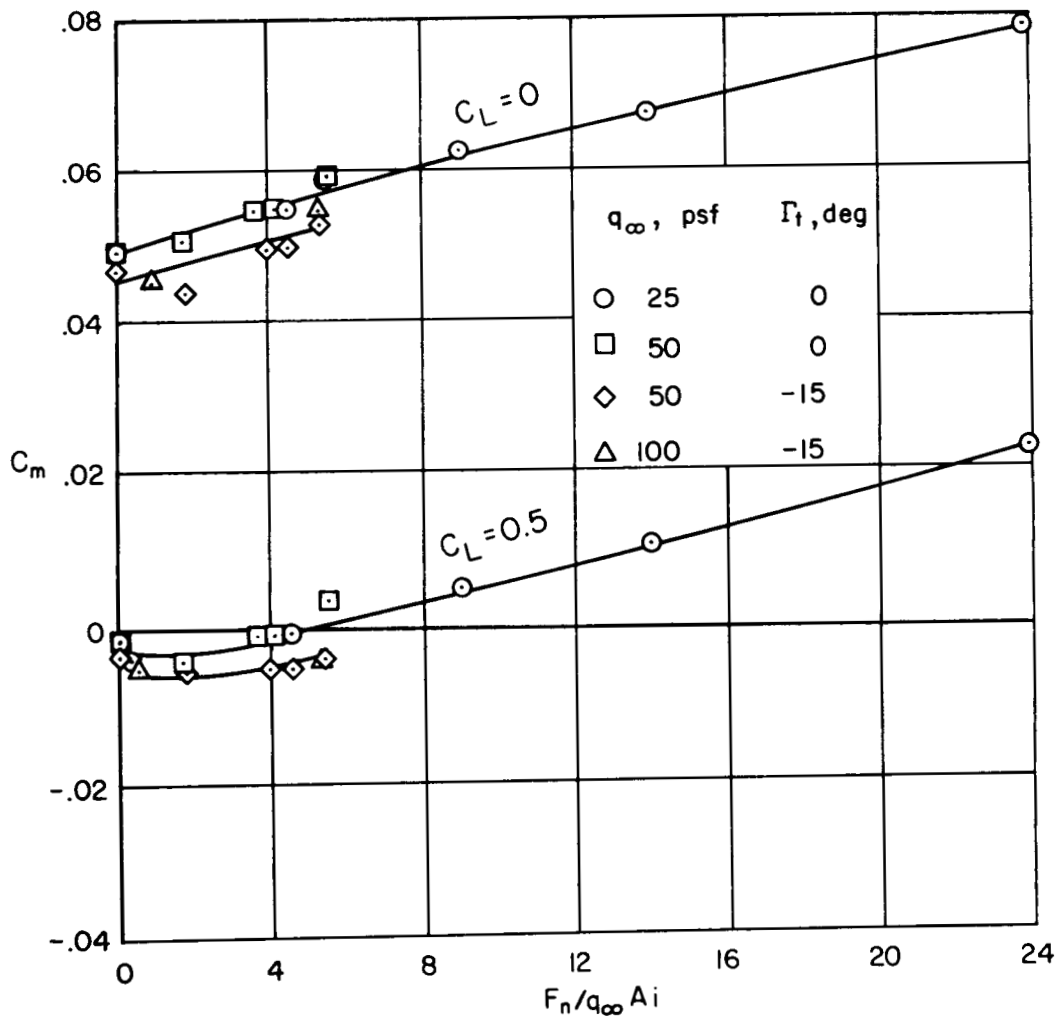

Figure 14.- The variation of pitching-moment coefficient with change in the parameter $F_n/q_\infty A_i$; $\delta_f = 0^\circ$, $i_t = -5^\circ$.

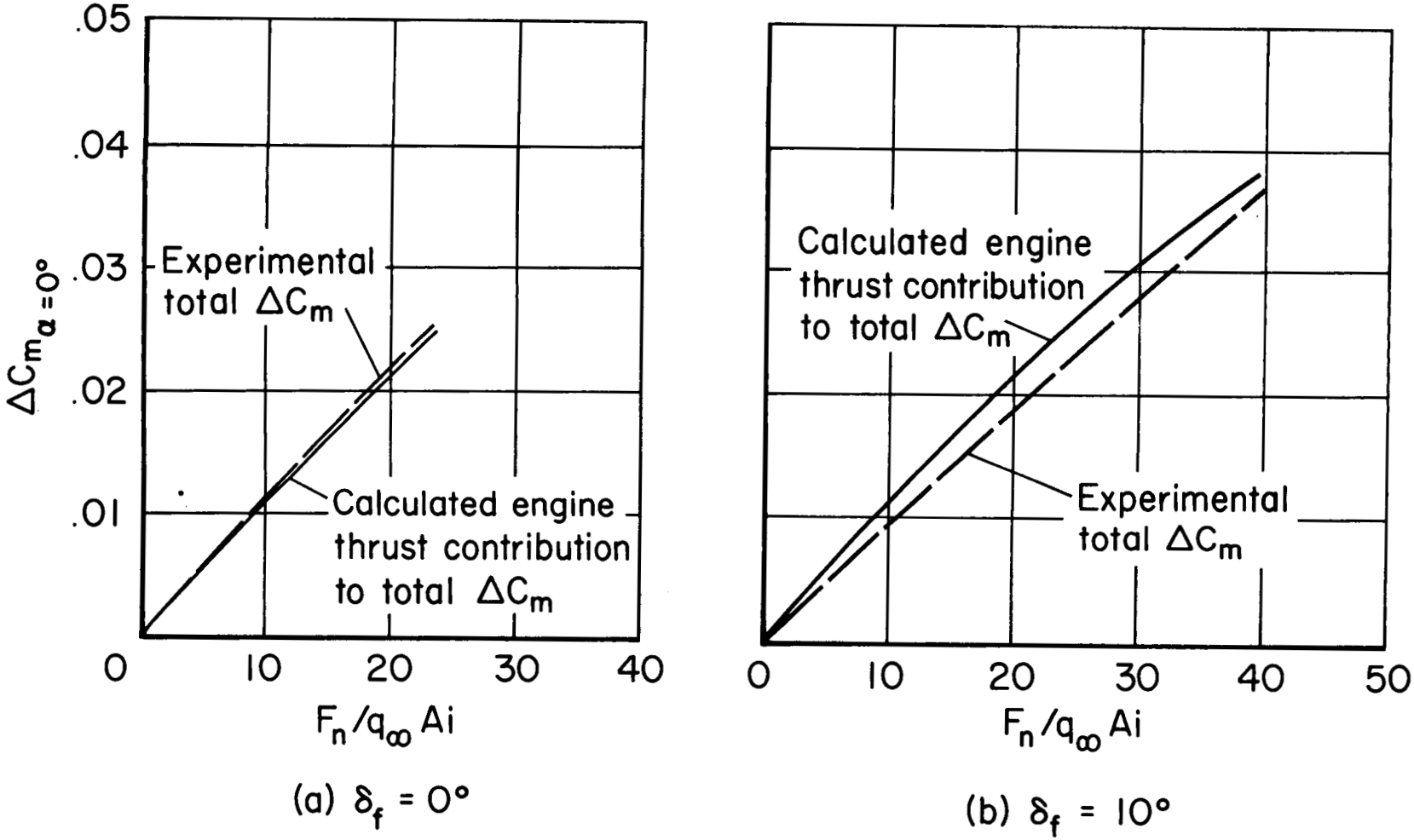

Figure 15.- The variation of pitching-moment increment with engine thrust; $\alpha = 0°$, $\Gamma_t = 0°$, $i_t = -5°$.

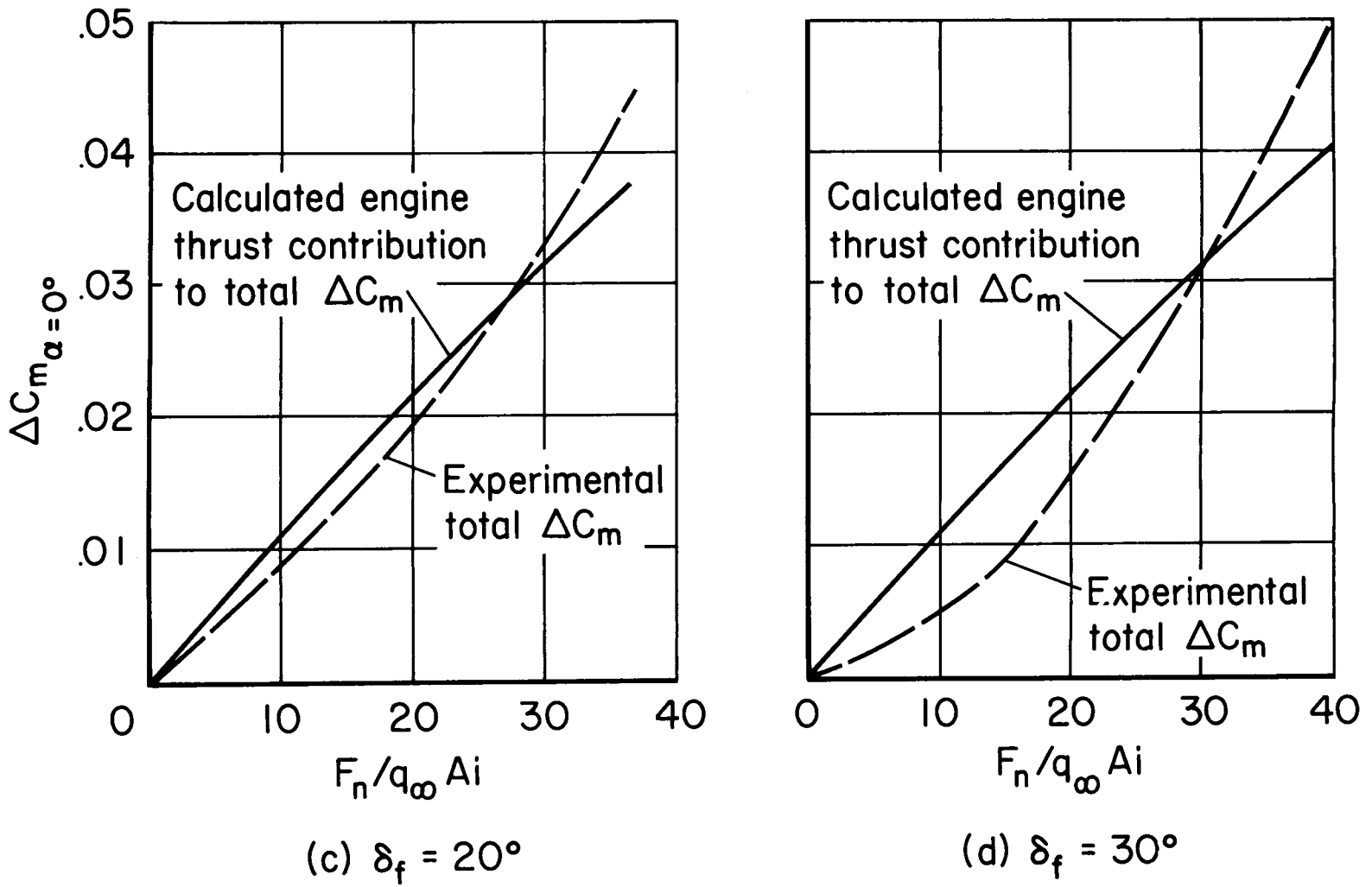

Figure 15.- Concluded.

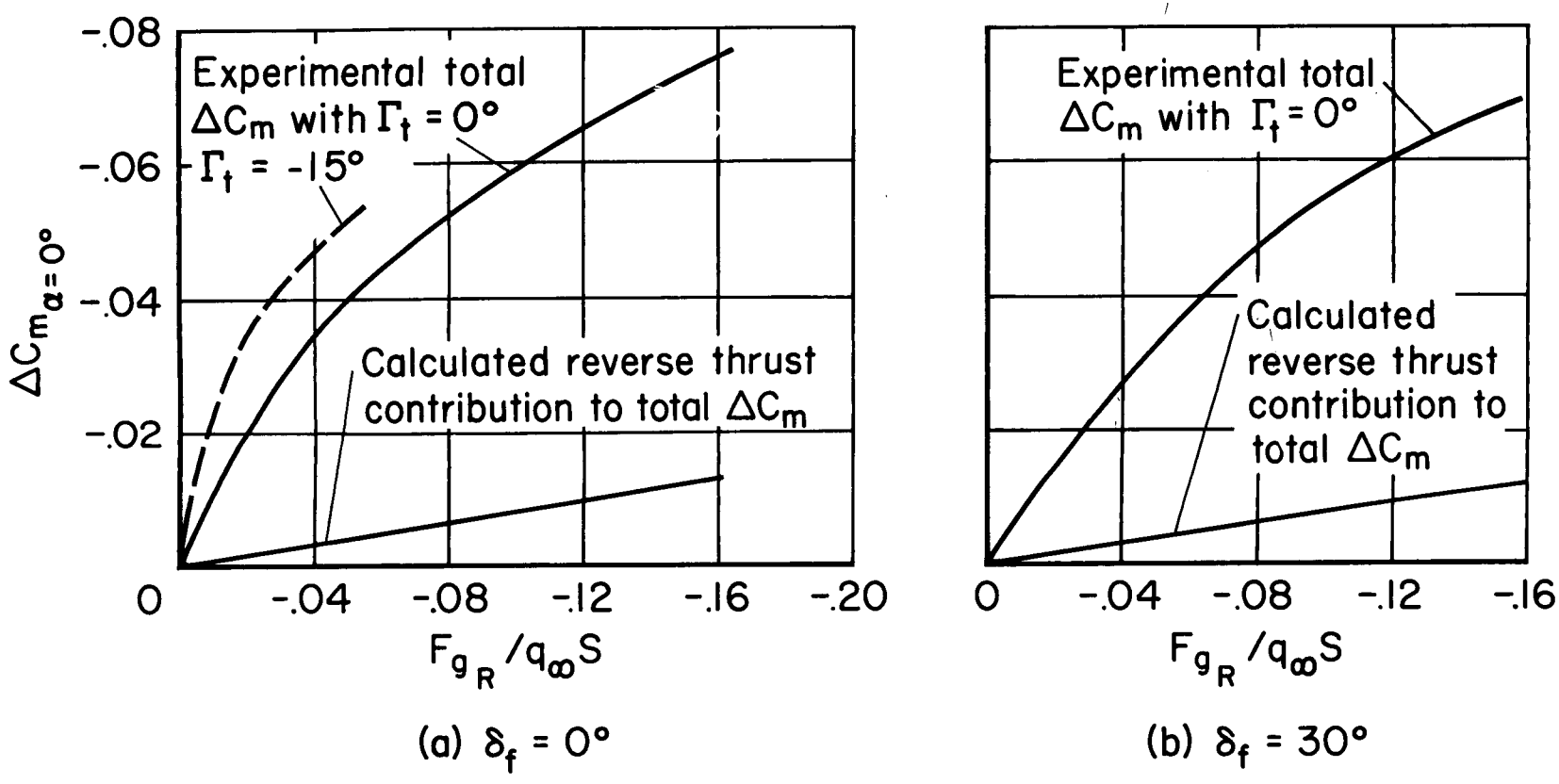

Figure 16.- The variation of pitching-moment increment with reverse thrust; $\alpha = 0°$, $i_t = -5°$.

[redacted]

8/8/67

"The aeronautical and space activities of the United States shall be conducted so as to contribute . . . to the expansion of human knowledge of phenomena in the atmosphere and space. The Administration shall provide for the widest practicable and appropriate dissemination of information concerning its activities and the results thereof."

—NATIONAL AERONAUTICS AND SPACE ACT OF 1958

NASA SCIENTIFIC AND TECHNICAL PUBLICATIONS

TECHNICAL REPORTS: Scientific and technical information considered important, complete, and a lasting contribution to existing knowledge.

TECHNICAL NOTES: Information less broad in scope but nevertheless of importance as a contribution to existing knowledge.

TECHNICAL MEMORANDUMS: Information receiving limited distribution because of preliminary data, security classification, or other reasons.

CONTRACTOR REPORTS: Technical information generated in connection with a NASA contract or grant and released under NASA auspices.

TECHNICAL TRANSLATIONS: Information published in a foreign language considered to merit NASA distribution in English.

TECHNICAL REPRINTS: Information derived from NASA activities and initially published in the form of journal articles.

SPECIAL PUBLICATIONS: Information derived from or of value to NASA activities but not necessarily reporting the results of individual NASA-programmed scientific efforts. Publications include conference proceedings, monographs, data compilations, handbooks, sourcebooks, and special bibliographies.

Details on the availability of these publications may be obtained from:

SCIENTIFIC AND TECHNICAL INFORMATION DIVISION

NATIONAL AERONAUTICS AND SPACE ADMINISTRATION

Washington, D.C. 20546

[redacted]